Therapeutic effect of α7 nicotinic receptor activation after ischemic stroke in rats

**Laura Aguado[1,2], Ana Joya[1,2], Maider Garbizu[1],
Sandra Plaza-García[2], Leyre Iglesias[1,3],
María Isabel Hernández[1], María Ardaya[1,4] ⓘ, Naroa Mocha[1],
Vanessa Gómez-Vallejo[2], Unai Cossio[2], Makoto Higuchi[5],
Alfredo Rodríguez-Antigüedad[6], Mari Mar Freijo[3,6],
María Domercq[1,7], Carlos Matute[1,7] ⓘ, Pedro Ramos-Cabrer[2,8],
Jordi Llop[2,9] and Abraham Martín[1,8]**

Abstract

Nicotinic acetylcholine α7 receptors (α7 nAChRs) have a well-known modulator effect in neuroinflammation. Yet, the therapeutical effect of α7 nAChRs activation after stroke has been scarcely evaluated to date. The role of α7 nAChRs activation with PHA 568487 on inflammation after brain ischemia was assessed with positron emission tomography (PET) using [^{18}F]DPA-714 and [^{18}F]BR-351 radiotracers after transient middle cerebral artery occlusion (MCAO) in rats. The assessment of brain oedema, blood brain barrier (BBB) disruption and neurofunctional progression after treatment was evaluated with T_2 weighted and dynamic contrast-enhanced magnetic resonance imaging (T_2 W and DCE-MRI) and neurological evaluation. The activation of α7 nAChRs resulted in a decrease of ischemic lesion, midline displacement and cell neurodegeneration from days 3 to 7 after ischemia. Besides, the treatment with PHA 568487 improved the neurofunctional outcome. Treated ischemic rats showed a significant [^{18}F]DPA-714-PET uptake reduction at day 7 together with a decrease of activated microglia/infiltrated macrophages. Likewise, the activation of α7 receptors displayed an increase of [^{18}F]BR-351-PET signal in ischemic cortical regions, which resulted from the overactivation of MMP-2. Finally, the treatment with PHA 568487 showed a protective effect on BBB disruption and blood brain vessel integrity after cerebral ischemia.

Introduction

Stroke is a devastating disease that represents the primary cause for sustained disability worldwide. Despite this, translational stroke medicine has largely failed in neuroprotection and in extending the maximal time windows of thrombolysis and mechanical thrombectomy for limiting brain ischemic injury.[1,2] Hence, the

[1]Achucarro Basque Center for Neuroscience, Leioa, Spain
[2]CIC biomaGUNE, Basque Research and Technology Alliance,
San Sebastian, Spain
[3]Neurovascular Group, Biocruces Health Research Institute, Barakaldo,
Spain
[4]Donostia International Physics Center (DIPC), San Sebastian, Spain
[5]National Institute of Radiological Sciences, National Institutes for
Quantum and Radiological Science and Technology, Chiba, Japan
[6]Department of Neurology, Cruces University Hospital, Barakaldo, Spain

[7]Department of Neuroscience, University of Basque Country
(UPV/EHU) and CIBERNED, Leioa, Spain
[8]Ikerbasque Basque Foundation for Science, Bilbao, Spain
[9]Centro de Investigación Biomédica en Red – Enfermedades
Respiratorias, CIBERES, Madrid, Spain

Corresponding author:
Abraham Martín, Achucarro Basque Center for Neuroscience, Science
Park of the UPV/EHU, 48940 Leioa, Spain.
Email: abraham.martin@achucarro.org

establishment of valid theragnostic biomarkers will contribute to accelerate the approval of new therapies for stroke.[3] Recent findings have shown the promising therapeutic potential and diagnostic perspectives of neuroreceptors as immune modulators in experimental stroke.[4] In fact, the overexpression of cholinergic receptors and particularly nicotinic acetylcholine α7 receptors (α7 nAChRs) on peripheral innate immune cells modulate inflammatory reaction following stroke.[5] In the ischemic brain, positron emission tomography (PET) with the radiotracer [^{11}C]NS14492, together with immunohistochemical studies showed the overexpression of α7 nAChRs in microglia and infiltrated macrophages as response to the ischemic insult. Besides, the activation of these receptors decreased the inflammatory reaction and the expression of selectines, adhesion molecules and infiltrated T lymphocytes, suggesting the key role of α7 nAChRs in the regulation of leucocyte infiltration into the ischemic tissue after stroke in rats.[6] In addition, recent *in vivo* studies have observed the therapeutic effect of nicotinic receptor agonists against blood brain barrier disruption (BBBd) and brain oedema induced by stroke and traumatic brain injury through the systemic cholinergic anti-inflammatory pathway.[7,8] Hence, current and future developments in the cross-talk between the immune stroke reaction and nicotinic receptor activation will likely identify novel avenues for treating stroke damage using agonists of α7 nAChRs.[5,9]

Our study aims to further investigate the therapeutic potential of α7 nAChRs on microglial/macrophage activation, matrix metalloproteases (MMPs) activation and BBBd using *in vivo* multimodal imaging, *ex vivo* cellular and molecular techniques and neurofunctional evaluation during the first week after ischemic stroke in rats. In particular, ischemic rats treated either with the selective α7 nAChR agonist PHA 568487 or vehicle were subjected to PET studies with [^{18}F]DPA-714 for translocator protein 18KDa (TSPO) imaging, as surrogate biomarker for inflammatory reaction, and [^{18}F] BR351 for the *in vivo* evaluation of MMPs activation after cerebral ischemia.[10,11] Additionally, the pharmacological activation of α7 nAChRs and its effects on brain damage, midline displacement and the BBBd evolution was studied with magnetic resonance imaging (MRI) and neurological evaluation. Finally, immunohistochemistry (IHC) together with gelatine zymography were used to evaluate TSPO expression on microglia/macrophages activation, neurodegenerative neurons, blood vascular integrity and MMPs with gelatinase activity.

The results reported here provide novel information about the role of α7 nAChRs on the subacute ischemic immune reaction and their therapeutic potential on brain damage progression, inflammation, brain matrix degradation and BBB integrity following experimental stroke. Hence, these findings may ultimately contribute to the establishment of novel nicotinic receptor-based theragnostic biomarkers and accelerate the development of new stroke therapies.

Materials and methods

Animal model and experimental set-up

Eight-weeks old -male Sprague-Dawley rats (n = 40; 305 ± 8.4 g body weight; Janvier, France) were used. 24 animals were included to experimental evaluations and a total of 16 rats were excluded, 8 rats due to absence of brain infarction with MRI evaluation at 24 hours after ischemia and 8 rats for mortality during early (minutes; 2 rats) or late (24 hours; 6 rats; 3 vehicle and 3 PHA-treated ischemic rats) reperfusion.

Animal experimental protocols and relevant details regarding welfare were approved by the Ethical Committee at CIC biomaGUNE and local authorities local authorities and were conducted in accordance with the Directives of the European Union on animal ethics and welfare (2010/63/UE). All studies were conducted in our AAALAC certified animal facilities. Finally, animal experiments were reported in accordance with the ARRIVE guidelines. Transient focal ischemia was produced under anaesthesia by a 75 min intraluminal occlusion of the middle cerebral artery (MCAO) followed by reperfusion as described previously.[12] Briefly, rats were anaesthetized with 2.5% isoflurane in 100% O_2 and a 2.6-cm length of 4-0 monofilament nylon suture was introduced into the right external carotid artery up to the level where the MCA branches out. Animals were then sutured and placed in their cages with free access to water and food. After 75 minutes, the animals were re-anesthetized and the filament was removed to allow reperfusion.

During 7 consecutive days, starting at 1 hour following MCAO, a first group of 12 rats was treated daily with intraperitoneal (i.p.) administration of *N*-(3*R*)-1-Azabicyclo [2.2.2]oct-3-yl-2,3-dihydro-1,4-benzodioxin-6-carboxamide fumarate (PHA 568487, selective α7 nAChR agonist; 1.25 mg/Kg) and a control ischemic group of 12 rats received the same daily volume of vehicle (physiologic saline solution) in a randomized and blinded fashion (Figure 1(a)). Both groups of ischemic rats (n = 24) were subjected to T_2-weighted (T_2W), Dynamic Contrast Enhanced (DCE)-MRI scans and neurological evaluation at 1, 3 and 7 days after reperfusion to evaluate the effect of the treatment on brain infarction volume, midline displacement, BBBd and neurological outcome. Following MRI studies, all animals (n = 24) were subjected at different time points to PET imaging of TSPO with [^{18}F]DPA-714 (n = 10) and matrix metalloproteinases (MMPs) with
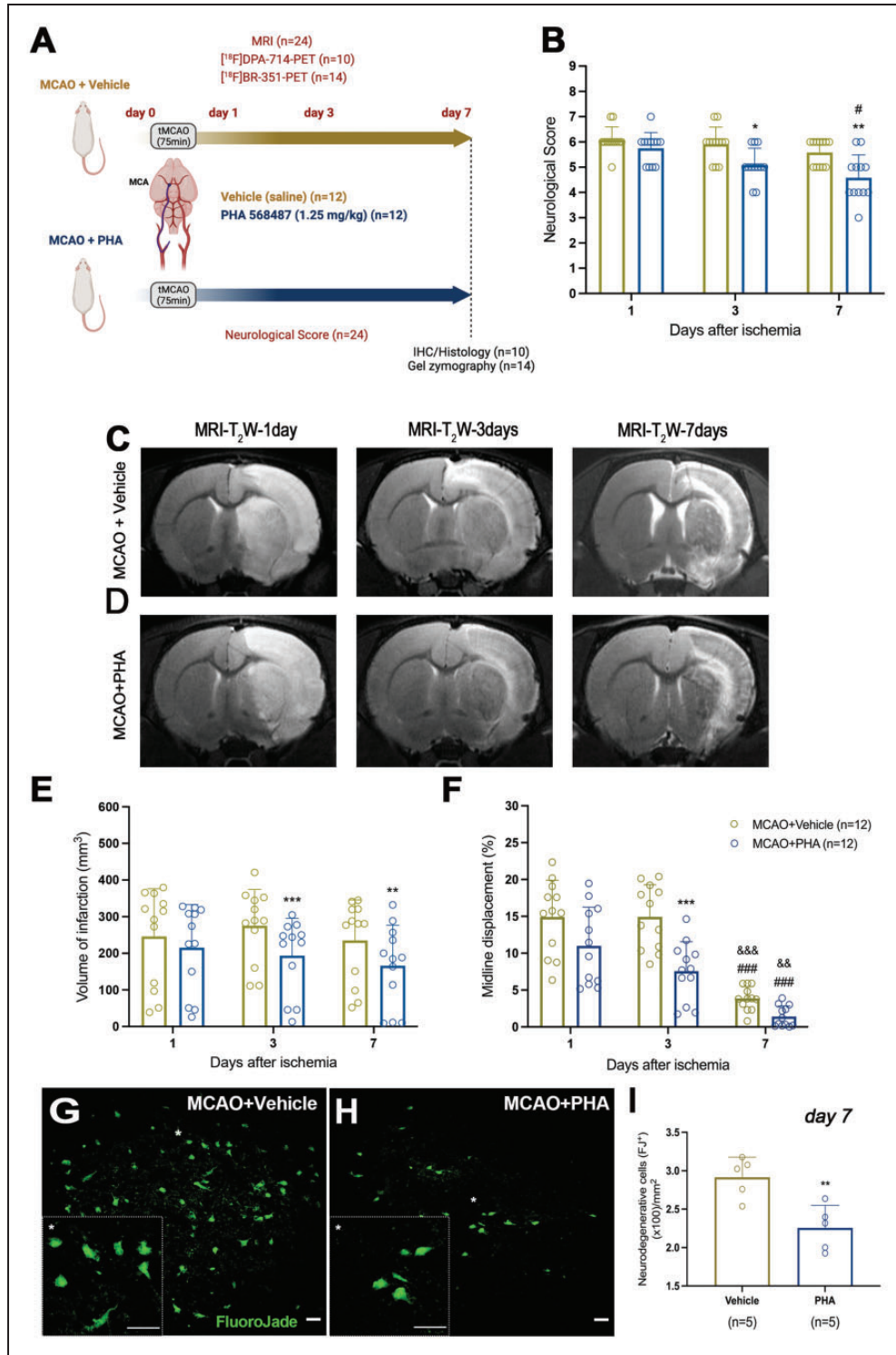
Figure 1. Experimental set-up of the therapeutic evaluation of α7 nicotinic receptor activation and MRI (T$_2$W) images of axial planes at the level of ischemic lesion after cerebral ischemic in vehicle and PHA treated rats (a, c–d). Neurological impairment (b), volume of infarction (e) and midline displacement (f) was evaluated at days 1, 3 and 7 after MCAO in vehicle (n = 12) and PHA-treated (n = 12) rats. Fluoro-Jade positive cells shows degenerative neurons in the ischemic region after MCAO in vehicle (n = 5) and PHA-treated (n = 5) rats (g–i). *p < 0.05, **p < 0.01 and ***p < 0.001 compared with vehicle; #p < 0.05 and ###p < 0.001 compared with day 1; &&p < 0.01 and &&&p < 0.01, compared with day 3. Scale bars, 20 μm. Values are presented as scatter dot blot (mean ± SD).

[^{18}F]BR351 (n = 14) to evaluate the effect of α7 nAChR activation on glial activation and MMP expression. All brains from animals subjected to imaging studies (n = 24) were used for ex vivo studies. *Ex vivo* ICH studies for TSPO and microglial activation, Fluoro-Jade staining (n = 10) and gel zymography (n = 14) were also performed on those animals to validate PET imaging findings (Figure 1(a)). Finally, both the neurological score and ex vivo analysis were performed in a blind fashion.

Magnetic resonance imaging

T$_2$W-MRI scans were acquired to evaluate the infarction volume in treated and control rats at days 1, 3 and 7 after ischemia onset. In addition, DCE-MRI scans during the first week after ischemia were carried out to assess the influence of treatment on BBBd after ischemia. Scans were performed in rats anaesthetized with isoflurane (2–2.5%) in a 30/70% mixture of O$_2$/N$_2$. Animals were placed into an MRI rat compatible holder and maintained in normothermia using a water-based heating blanket at 37°C. To ensure animal welfare, temperature and respiration rate were continuously monitored while they remained in the MRI scanner, using a SAII M1030 system (SA Instruments, NY, USA). MRI *in vivo* studies were performed on a 7T horizontal bore Bruker Biospec USR 70/30 MRI system (Bruker Biospin GmbH, Ettlingen, Germany), interfaced to an AVANCE III console, and with a BGA12-S imaging gradient insert (maximal gradient strength 400 mT/m, switchable within 80 μs). Measurements were performed with a 72 mm volumetric quadrature coil for excitation and a 20 mm rat brain surface coil for reception. The imaging session started with the acquisition of a scout scan, which was used to plan the whole study focusing on the region of interest. T$_2$W images were acquired with a Bruker's RARE (Rapid Acquisition with Relaxation Enhancement) sequence (Effective TE = 40 ms, TR = 4400 ms, NA = 2; Matrix = 256 × 256 points; FOV = 25.6 × 25.6 mm; spatial resolution = 100 × 100 μm; 24 contiguous slices of 1 mm thickness covering the whole brain), which was used to quantify the volume of the lesion.

For the evaluation of BBB integrity, the tail vein was catheterized with a 24-gauge catheter for intravenous administration of the contrast agent (Multihance, 0.2 mmol/ml, 1 ml/Kg body weight). The BBBd was assessed using DCE-MRI, which allowed to differentiate between changes in vascular permeability and changes in the extravascular extracellular space (EES). The T$_1$-weighted (T$_1$W) DCE-MRI was acquired with a Bruker's FLASH (Fast low-angle shot) sequence (TE = 2.5 ms; TR = 31.25 ms; FA = 15°; NA = 1; NR = 200; Matrix = 128 × 128 points; FOV = 25.6 × 25.6 mm;

spatial resolution = 200 × 200 μm; 5 slices of 1 mm thickness covering the ischemic lesion). This technique involves the serial acquisition in rapid succession of MR images (NR = 200) of a tissue of interest, being the ischemic lesion in this particular case, before and after the intravenous administration of Multihance, a gadolinium-based paramagnetic contrast agent. DCE-MRI allows to monitor changes in the T1 relaxation rate of the tissue after the administration of gadolinium with repeated serial imaging using T$_1$W images.

Magnetic resonance imaging analysis

For image analysis, regions of interest (ROIs) were manually defined using the Image J (Version 1.53k, NIH) software. The calculation of the lesion volume using MRI was carried out by summing the areas of infarcted regions showing hyperintense signals of all slices affected by the lesion. The evaluation of midline displacement in the entire brain was assessed using the following formula ((*Volume of ipsilateral hemisphere/Volume of contralateral hemisphere*)-1) * 100. BBB permeability (ktrans) maps were obtained from five DCE-MRI images with DCE@urLAB software[13] in the lesion volume measured with T$_2$W-MRI, using the Tofts Model with the following input parameters: T10 (tissue) pixel-wise obtained from acquired T1 maps, T10 blood = 2070 ms,[14] TR = 31.25 ms, FA = 15°, frame period = 2 s, N° frames = 200, contrast agent relaxivity = 4.24 mM^{-1} s^{-1}, hematocrit = 0.43, Injection frame, Frames for initial area under the curve (IAUC) = 5 and Arterial Input Function (AIF) as measured from a region of interest located at the carotid artery.

Radiochemistry

The production and quality control of [^{18}F]DPA-714 (non-decay corrected radiochemical yield = 11 ± 2%; radiochemical purity >95% at the time of injection; molar activity values 160–430 GBq/μmol at the end of the synthesis (EOS)) was carried out following established protocols in our laboratory.[15] [^{18}F]BR351 was carried out following a previously published method with minor modifications.[16] Radiochemical purity was always >95% at the time of injection, and molar activity values were in the range 90–220 GBq/μmol (EOS). This experimental procedure is described in detail in the Supporting Information.

Positron emission tomography scans and data acquisition

PET scans were performed using an eXplore Vista PET-CT camera (GE Healthcare, Waukesha, WI, USA). Scans were performed in rats anaesthetized with 2–2.5% of isoflurane in 100% O$_2$. Animals were

placed into a rat holder compatible with the PET acquisition system and maintained in normothermia using a water-based heating blanket at 37°C. To ensure animal welfare, temperature and respiration rate were continuously monitored while they remained in the PET camera, using a SAII M1030 system (SA Instruments, NY, USA). The tail vein was catheterized with a 24-gauge catheter for intravenous administration of the radiotracers. For evaluation of treatments on TSPO binding after ischemia, [18F]DPA-714 was injected concomitantly with the start of the PET acquisition and dynamic brain images were acquired for 30 min using 23 frames (3×5, 3×15, 4×30, 4×60, 4×120, 5×180 s) in the 400–700 keV energetic window. For the evaluation of MMP expression, the radiotracer [18F]BR351 was injected into the tail vein and after an uptake period of 100 min, rats were anesthetized and placed on the PET camera for 30 min brain static acquisition. After each PET scan, CT acquisitions were also performed (140 mA intensity, 40 kV voltage), to provide anatomical information of each animal as well as the attenuation map for the later PET image reconstruction. Dynamic and static acquisitions were reconstructed (decay and CT-based attenuation corrected) with filtered back projection (FBP) using a Ramp filter with a cut-off frequency of $0.5 \, mm^{-1}$.

Positron emission tomography image analysis

PET images were analysed using PMOD image analysis software (Version 3.5, PMOD Technologies Ltd, Zurich, Switzerland). For the analysis of PET signal, both PET images and an MRI (T_2W) rat brain template from Pmod were separately manually co-registered to the CT of the same animal to generate a spatial normalization. Subsequently, MRI brain template was automatically co-registered to PET images. Volumes of Interest (VOIs) were manually drawn in the entire ipsilateral and contralateral hemispheres, cerebral cortex and the striatum on slices of the MRI (T_2W) images for each animal to study the whole brain [18F]DPA-714 and [18F]BR351 PET signals. For dynamic PET scans, the last five ([18F]DPA-714) frames were used to calculate radiotracer uptake over the last 15 min. For static PET scans, the 30 min frame was used to quantify the [18F]BR351 uptake. Average values in each VOI were determined and expressed as percentage of injected dose per cubic centimetre (%ID/cc).

Immunohistochemistry and Fluoro-Jade staining.
Immunohistochemistry (IHC) and Fluoro-Jade staining were carried out at day 7 after imaging studies in animals treated with PHA568487 and vehicle. The brain was removed, frozen and cut in 6-μm-thick sections in a cryostat. For IHC, sections were fixed,

washed and permeabilized. For antigen retrieval, sections were incubated in antigen unmasking citrate-based (Vector laboratories, California, USA) solution. After washing, samples were saturated with a solution of bovine serum albumin (BSA) and incubated during 2 h at room temperature with primary antibodies. The first set of sections were stained for TSPO with a rabbit anti-TSPO (NP155, 1:1000) and for CD11b with mouse anti-CD11b (1:300; Serotec, Raleigh, NC, USA). Finally, the second set of sections were stained for VE-Cadherin with rabbit anti-VE-Cadherin (1:50; Thermo Fisher, Madrid, Spain) and for GFAP with chicken anti-GFAP (1/500; AbCam, Cambridge, UK). Sections were washed, incubated with secondary antibodies Alexa Fluor 488 goat anti-rabbit IgG, Alexa Fluor 594 goat anti-mouse IgG and Alexa Fluor 647 goat anti-chicken IgY (Molecular Probes, Life Technologies, Madrid, Spain, 1:1000), and mounted with a prolong antifade kit with or without DAPI in slices (Molecular Probes Life Technologies, Madrid). For Fluoro-Jade, sections were dried at room temperature, and rehydrated. Fluorescent background blocking was performed with potassium permanganate. Samples were stained with Fluoro-Jade C (Millipore, California, USA) staining solution and washed again. Sections were dried overnight at room temperature, cleared using xylene and mounted with DPX (Sigma-Aldrich, Spain). Standardized images acquisition was performed with Axio Observer Z6 (Zeiss, Tres Cantos, Spain) for TSPO/CD11b, the Leica TCS SP8 STED 3X microscope for Fluoro-Jade and the Leica Stellaris confocal microscope (Hospitalet de Llobregat, Spain) for VE-Cadherin/GFAP imaging. Cells were counted in ten representative and different fields defined manually in both ischemic cortex and striatal regions at 20x magnifications by using Image J (Version 1.53k, NIH, USA) software. This experimental procedure is described in detail in the Supporting Information.

Gel zymography

Tissues were homogenized with lysis buffer and centrigugated at 12,500 rpm for 5 min at 4°C, the supernatants were used for extraction of gelatinolytic activity. Same concentration of protein in 500 μL of lysis buffer was incubated with 50 μL of gelatine-sepharose (Gelatin Sepharose 4B, GE Healthcare, Uppsala, Sweden). Subsequently, the pellet with gelatine-sepharose was washed with 500 μL of washing buffer and centrifuged before the separation of gelatinases with 150 L of elution buffer. Protein extracts (10 μL) were loaded in 10% acrylamide gels containing porcine gelatine (10 mg/ml) and human MMP-9 (Calbiochem, Madrid, Spain) was used as the gelatinase standard. After electrophoresis, gels were washed in H_2Od, rinsed three times and

incubated for 48 h at 37°C in incubation buffer. After incubation, gels were stained in a solution of 0.1% amido black in acetic acid, methanol and H_2Od for 1 h and unstained. Finally, the gels were imaged and analysed to determine intensity of the bands (ChemiDoc and Image Lab software, BioRad, Alcobendas, Spain). This experimental procedure is described in detail in the Supporting Information.

Neurological assessment

The assessment of neurological outcome induced by cerebral ischemia was based on a previously reported 9-neuroscore test.[17] This test is a global neurological assessment that was developed to measure neurological impairments following stroke and assesses a variety of motor, sensory and reflex responses. Before imaging evaluations, four consecutive tests were performed at days 1, 3 and 7 after ischemia in treated and control rats as as described previously.[12]

Statistical analyses

The effects of the treatment in infarct volume, midline displacement, BBBd and PET uptake within each brain region at days 1, 3 and 7 after cerebral ischemia were averaged and compared with the averaged values of every time point using repeated measures two-way ANOVA followed by Tukey's multiple-comparison tests for post-hoc analysis. Likewise, the neurological outcome at different days after cerebral ischemia were averaged and compared with the averaged values of every time point using the same statistical method as above. For immunohistochemical and gel zymography studies, microglial/TSPO cells and intensity of MMP bands after treatments (7 days after MCAO) were averaged and compared using repeated measures one-way ANOVA followed by Tukey's multiple-comparison tests for post-hoc analysis. Finally, the effect of the α7 nAChR agonist in the activation of ipsilateral MMP-2 active form and Fluoro-Jade positive cells were compared using unpaired t-Test. The level of significance was regularly set at $P < 0.05$. Normality of data was tested using Shapiro-Wilk test. Statistical analyses were performed with GraphPad Prism version 9 software.

Results

Effect of α7 nAChRs activation on stroke outcome and neurodegeneration

The role of α7 nicotinic receptors on neurological outcome, stroke evolution, BBBd, inflammatory reaction and MMP expression after ischemia was explored using *in vivo* advanced imaging, neurological evaluation, immunohistochemistry and zymography after the daily treatment (from day 0 to day 6) with the selective α7 nAChR agonist PHA 568487 and vehicle (Figure 1(a)).

Neurofunctional impartment including motor, sensory and reflex deficits was evaluated with the 9-neuroscore test at 1, 3 and 7 days after MCAO and treatments (Figure 1(b)). Both experimental groups of rats presented similar neurological impairment at day 1 after ischemia followed by a significant neurological outcome improvement at days 3 ($p < 0.05$) and 7 ($p < 0.01$) in PHA-treated ischemic rats compared to control ischemic animals (Figure 1(b)). Besides, the pharmacological activation of α7 nicotinic receptors with PHA showed a significant neurofunctional improvement at day 7 in relation to day 3 after MCAO ($p < 0.05$, Figure 1(b)).

Hyperintense regions of T_2W-MRI images showing the evolution of vasogenic oedema as the result of the ischemic infarction were evaluated at days 1, 3 and 7 in PHA and vehicle-treated ischemic rats (Figures 1(c) and (d)). Infarct volumes showed non-significant differences between both experimental groups of animals at day 1, followed by a significant infarct reduction at days 3 ($p < 0.001$) and 7 ($p < 0.01$, Figure 1(e)) in PHA + MCAO rats versus control ischemic animals. The effect of brain oedema on intracranial pressure was evaluated with the midline shift of brain tissue across the centre line of the brain (Figure 1(f)). Brain oedema following cerebral ischemia caused a midline displacement of circa 15% at days 1 and 3 followed by a significant reduction during the following seven days after MCAO ($p < 0.001$, Figure 1(f)). Likewise, the daily treatment with PHA limited the formation of brain oedema reducing the midline shift at day 3 ($p < 0.001$, Figure 1(f)) in relation to vehicle-treated ischemic animals.

Finally, the effect of the treatment on neurodegeneration was assessed by Fluoro-Jade staining that displayed a significant reduction in number of neurodegenerative cells at day 7 after ischemia in relation to control ischemic rats ($p < 0.01$, Figures 1(g) to (i)).

Role of α7 nAChRs on inflammatory reaction and MMP activation after MCAO

The role of α7 nicotinic receptors on inflammatory reaction and MMP activation was explored with PET imaging of TSPO and MMP activity using the radiotracers [18F]DPA-714 (TSPO ligand) and [18F]BR-351 (MMP activation), at days 1, 3 and 7 after daily treatment with PHA and vehicle. All images were quantified in standard units (%ID/cc). Co-registered axial brain images of [18F]DPA-714 and [18F]BR-351 PET brain signals to T_2W-MRI in PHA and vehicle treated ischemic rats sowed spatial-temporal inflammatory and

MMP activation changes in the region of the infarction at different days after reperfusion (Figures 2 and 4).

In the ipsilateral (ischemic) hemisphere, [^{18}F]DPA-714-PET showed a progressive signal increase from days 1 to 7 (p < 0.01 at day 7 vs day 1, Figure 2(e)) in vehicle + MCAO rats. Likewise, the treatment significantly reduced the inflammatory reaction over time showing significant differences at day 7 after MCAO in relation to control ischemic rats (p < 0.05, Figure 2(e)). Conversely, the contralateral hemispheres showed pseudo-control values at different days in both PHA and vehicle-treated rats (Figure 2(f)). Similarly to the ipsilateral whole brain hemisphere, infarcted cortex showed a significant [^{18}F]DPA-714 PET signal uptake at day 7 in PHA ischemic rats versus control animals (p < 0.05, Figure 2(e)) that was not observed in striatal region (Figure 2(h)).

Immunofluorescence staining studies displayed TSPO over-expression (in green; Figure 3(b)) in CD11b$^+$ cells (microglia/macrophages) after ischemia (in red; Figure 3(a)) in vehicle and PHA treated rats (Figures 3(a) to (d)). At day 7, the ischemic lesion showed an increase in the number of reactive microglia/macrophages expressing TSPO (in green and red; Figure 3(d)) in relation to contralateral regions (p < 0.01, p < 0.001, Figure 3(e) to (g)). Besides, the number of TSPO$^+$/CD11b$^+$ cells showed a significant decrease in both ipsilateral whole brain and cerebral cortex of PHA-treated animals in comparison with control ischemic rats (p < 0.01, Figures 3(e) and (f)). In contrast, the activation of α7 nAChRs with PHA showed a non-significant decline of the TSPO expression in striatal microglia/macrophages supporting those findings observed with *in vivo* PET imaging (Figure 3(g)).

PET imaging of *in vivo* MMP activation with [^{18}F]BR-351 showed the highest signal uptake at 24 hours in the entire region of the infarction followed by a slight decline from days 3 to 7 days (p < 0.05 versus day 1, Figures 4(b) and (e)). Likewise, PHA-treated rats displayed a non-significant MMP activation increase at days 3 and 7 after ischemia in relation to control ischemic animals (Figures 4(b), (d) and (e)). The regional distribution of [^{18}F]BR-351 in the ischemic territory showed different signal uptake (ipsilateral/contralateral of %ID/cc) for both cerebral cortex and striatum along the reperfusion (Figures 4(f) and (g). Firstly, the cerebral cortex showed similar [^{18}F]BR-351 signal ratios at day 1 for both experimental conditions followed by a significant increase of MMP activation from day 3 to 7 after MCAO in PHA-treated compared to control ischemic rats (p < 0.05, p < 0.01, Figure 4(f)). Secondly, the ischemic striatum showed higher PET signal ratios at different time points compared to those shown by cerebral cortex (Figure 4(g)). At day 1, control ischemic animals displayed highest values (circa 1.8 ipsi/contra

ratio of %ID/cc) followed by a progressive decline during the following week after ischemia (p < 0.01, Figure 4(g)). Finally, contrary to what was observed in the cerebral cortex, treated animals with PHA showed non-significant [^{18}F]BR-351 uptake differences in striatal region versus vehicle + MCAO rats.

The increase of MMP-9 (bands a and b, corresponding to 95 and 88 kDa) and MMP-2 (bands a and b, corresponding to 72 and 67 kDa) gelatinase activities at day 7 following cerebral ischemia and treatments was carried out with the semiquantitative analysis of the gelatine zymography (Figure 5(a) and S1). The zymogram analysis showed a non-significant increase of the band a (proenzyme) of MMP-9 in PHA-treated ischemic brains compared to both control ischemic and contralateral brain hemispheres (Figure 5(b)). In addition, the band b (active form) of MMP-9 displayed similar intensity values for both experimental conditions and brain hemispheres after ischemia (Figure 5(c)). Conversely, MMP-2 proenzim and active form increased significantly in the ischemic territory compared with contralateral hemispheres of both PHA and vehicle treated rats (p < 0.05, p < 0.01 and p < 0.001, Figures 5(d) and (e)). Finally, the active form of MMP-2 displayed a significant increase as response to PHA treatment in relation to vehicle + MCAO rats (p < 0.05, Figure 5(e)) supporting the *in vivo* MMP activation increase observed with [^{18}F]BR-351 PET imaging.

Therapeutic properties of α7 nicotinic receptor activation on BBBd after cerebral ischemia

The effect of the treatment on BBBd was assessed using T$_2$W and DCE-MRI at days 1, 3 and 7 after cerebral ischemia in the whole ischemic hemisphere, cerebral cortex and striatum (Figure 6). Serial brain-MRI images of a representative MCAO + vehicle and MCAO + PHA rats showed the extension of the ischemic lesion and BBBd (Ktrans) at the level of the lesion seven days after ischemic stroke (Figures 6(a) and (b)). Both experimental groups of animals experienced a similar progressive BBBd increase from day 1 to 3 after cerebral ischemia. At day 7, vehicle-treated rats showed the highest Ktrans value compared to days 1 and 3, that was reduced by the daily treatment with PHA (Figures 6(c) to (e)). In fact, results showed a significant decline of Ktrans values in the cerebral cortex by PHA treatment at day 7 after MCAO (p < 0.05, Figure 6(d)) confirming the protective role of α7 nicotinic receptors on BBB integrity.

Additionally, the *ex vivo* evaluation of the blood vascular integrity after ischemia was assessed in the cerebral cortex with immunohistochemistry to visualize
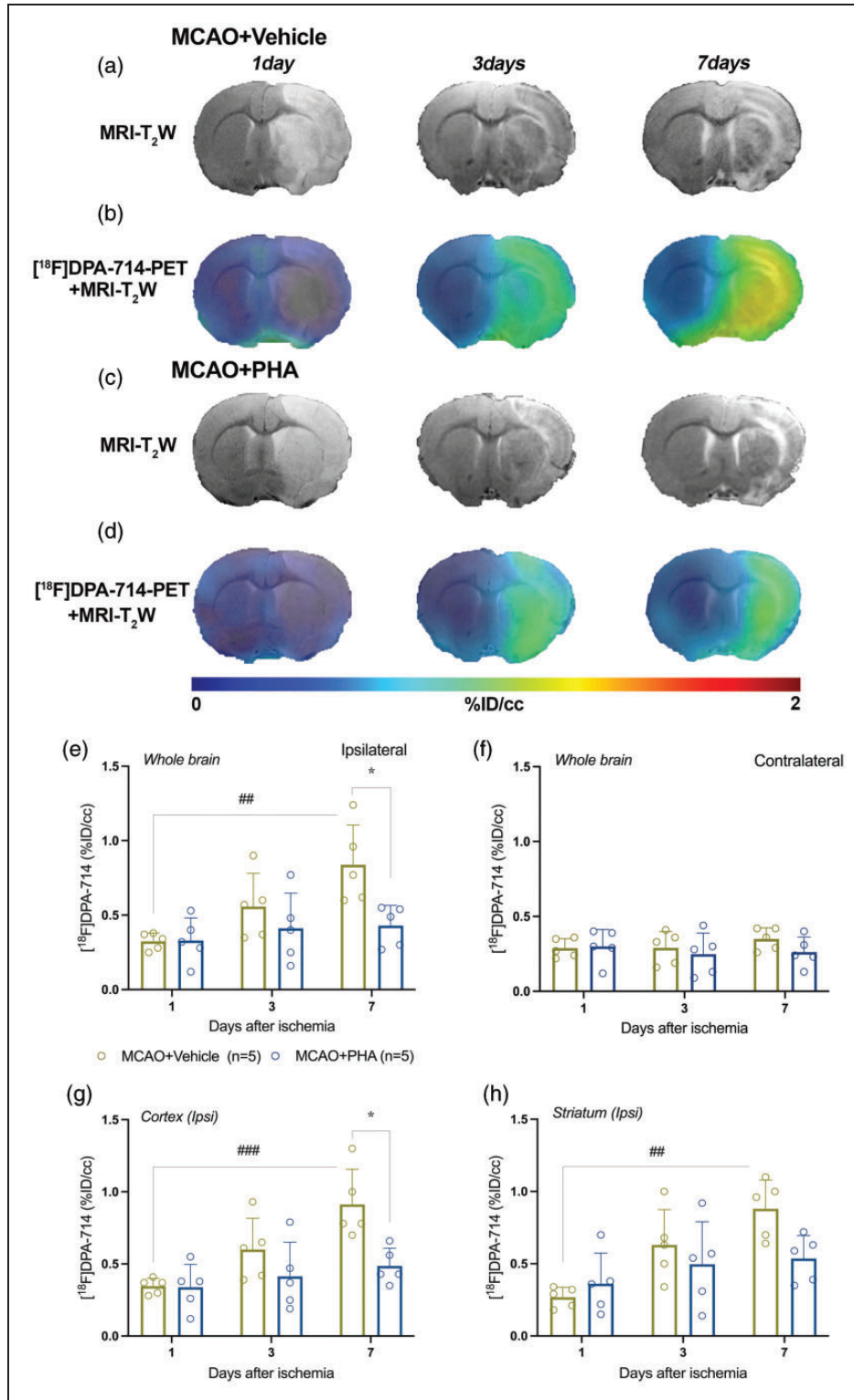
Figure 2. MRI-T$_2$W and PET images of [^{18}F]DPA-714 at days 1, 3 and 7 after MCAO in vehicle and PHA-treated rats. MRI (T$_2$W) (a, c) and TSPO receptor PET signal (b, d) images of axial planes at the level of the ischemic lesion. [^{18}F]DPA-714 PET signal was quantified at days 1, 3 and 7 after ischemia in the entire ipsilateral (e) and contralateral (f) cerebral hemisphere, ipsilateral cortex (g) and striatum (h). *p < 0.05 compared with vehicle; ##p < 0.01 and ###p < 0.001 compared with day 1. Values are presented as scatter dot blot (mean ± SD).
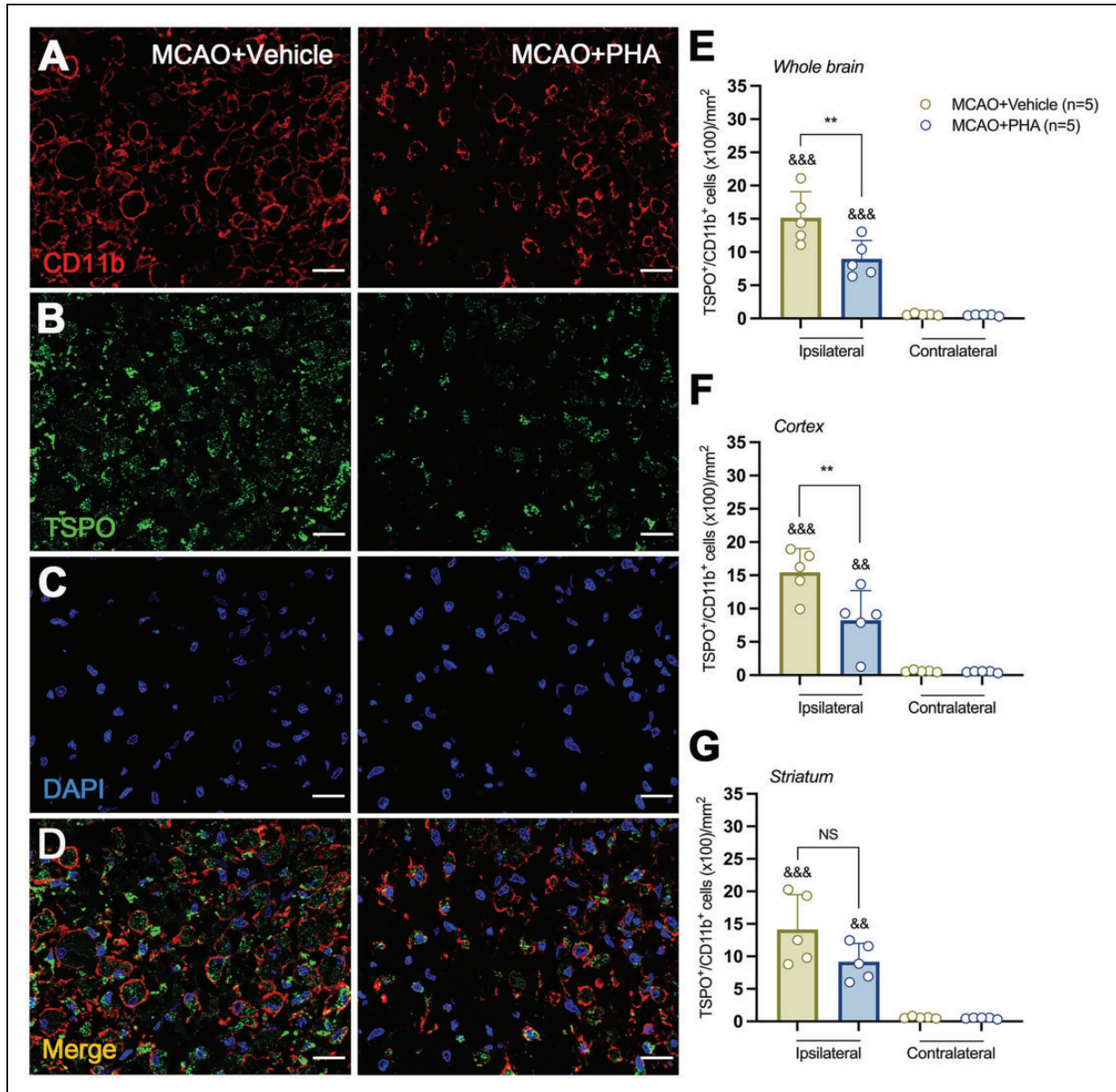
Figure 3. Immunofluorescent labeling of TSPO (green), CD11b (red) and DAPI (blue) in the ischemic area, shown as three channels. The data show TSPO expression in microglia/macrophages at day 7 after MCAO in and PHA-treated rats. CD11b-reactive microglia/macrophages (a) expressing TSPO expression (b) decrease after MCAO in PHA-treated rats in merged images of two immunofluorescent antibodies (d). The number of CD11b-reactive microglia/macrophages expressing TSPO was evaluated at day 7 in ipsilateral and contralateral whole brain (e), cortex (f) and striatum (g) after daily treatment with vehicle ($n = 5$) and PHA ($n = 5$). $**p < 0.01$ and $***p < 0.01$ compared with vehicle; $^{\&\&}p < 0.01$ and $^{\&\&\&}p < 0.001$ compared with contralateral. Scale bars, 20 μm. Values are presented as scatter dot blot (mean ± SD).

both VE-Cadherin and astrocytes (in green and pink, respectively; Figures 6(f) and (g)). Immunofluorescence showed a decrease of co-localized VE-cadherin (major determinant of endothelial cell contact integrity) and GFAP staining in vehicle + MCAO animals at day 7 after cerebral ischemia evidencing the loss of the blood vessel structure and neurovascular unit (Figure 6(f)).

Conversely, the pharmacological treatment with PHA protected the blood brain vessel integrity from ischemic injury as observed by VE-cadherin and GFAP blood vessel staining in the ischemic cortical territory (Figure 6(g)). Hence, altogether both *in vivo* and *ex vivo* findings evidenced the therapeutic effect of PHA treatment on BBB dysfunction after cerebral ischemia in rats.
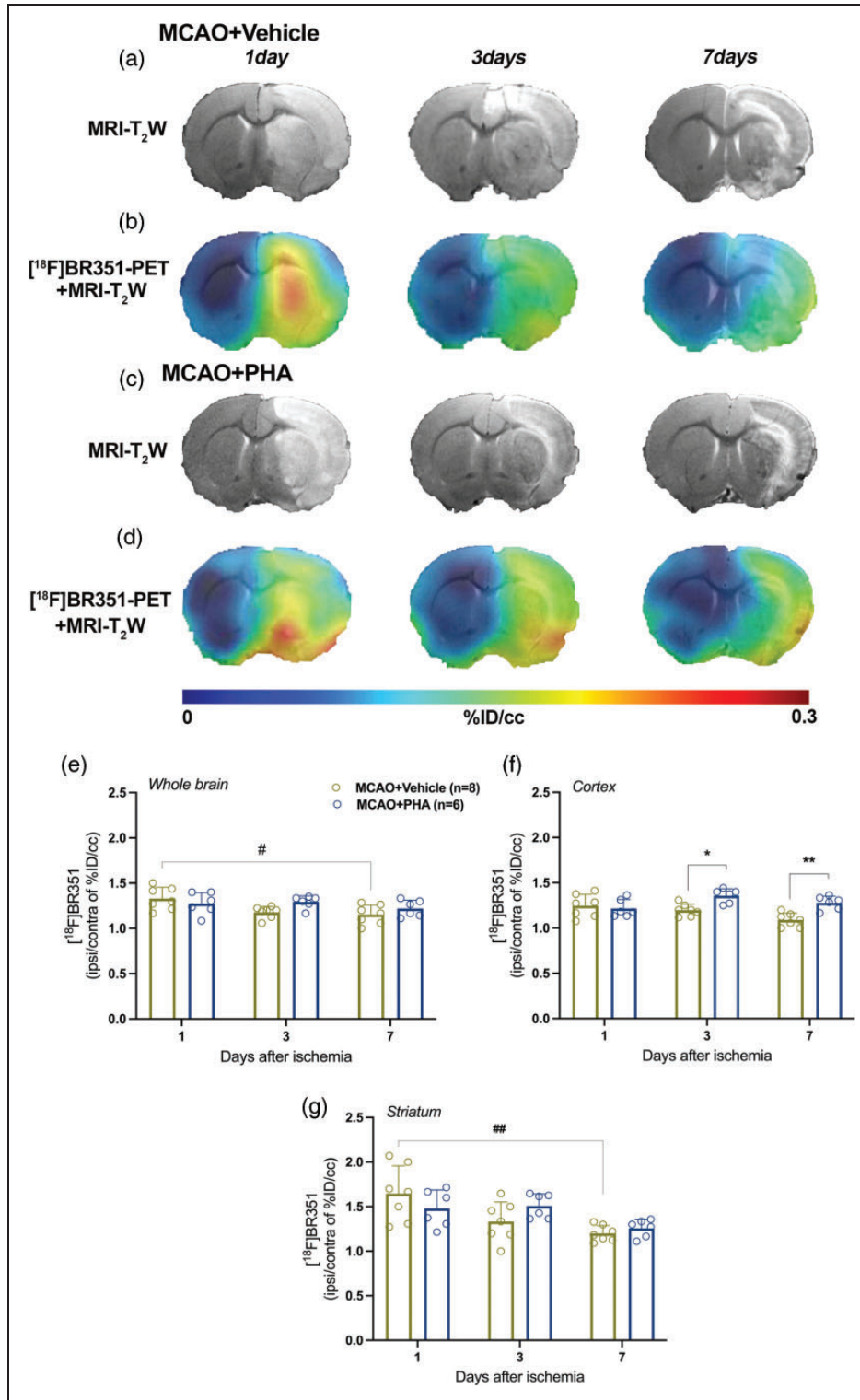
Figure 4. MRI-T$_2$W and PET images of [^{18}F]BR-351 at days 1, 3 and 7 after MCAO in vehicle and PHA-treated rats. MRI (T$_2$W) (a, c) and MMP PET signal (b, d) images of axial planes at the level of the ischemic lesion. [^{18}F]BR-351 PET signal was quantified at days 1, 3 and 7 after ischemia in the whole brain (e) cortex (f) and striatum (g). *p < 0.05 compared with vehicle; $^{##}$p < 0.05 and $^{##}$p < 0.01 compared with day 1; Values are presented as scatter dot blot (mean ± SD).
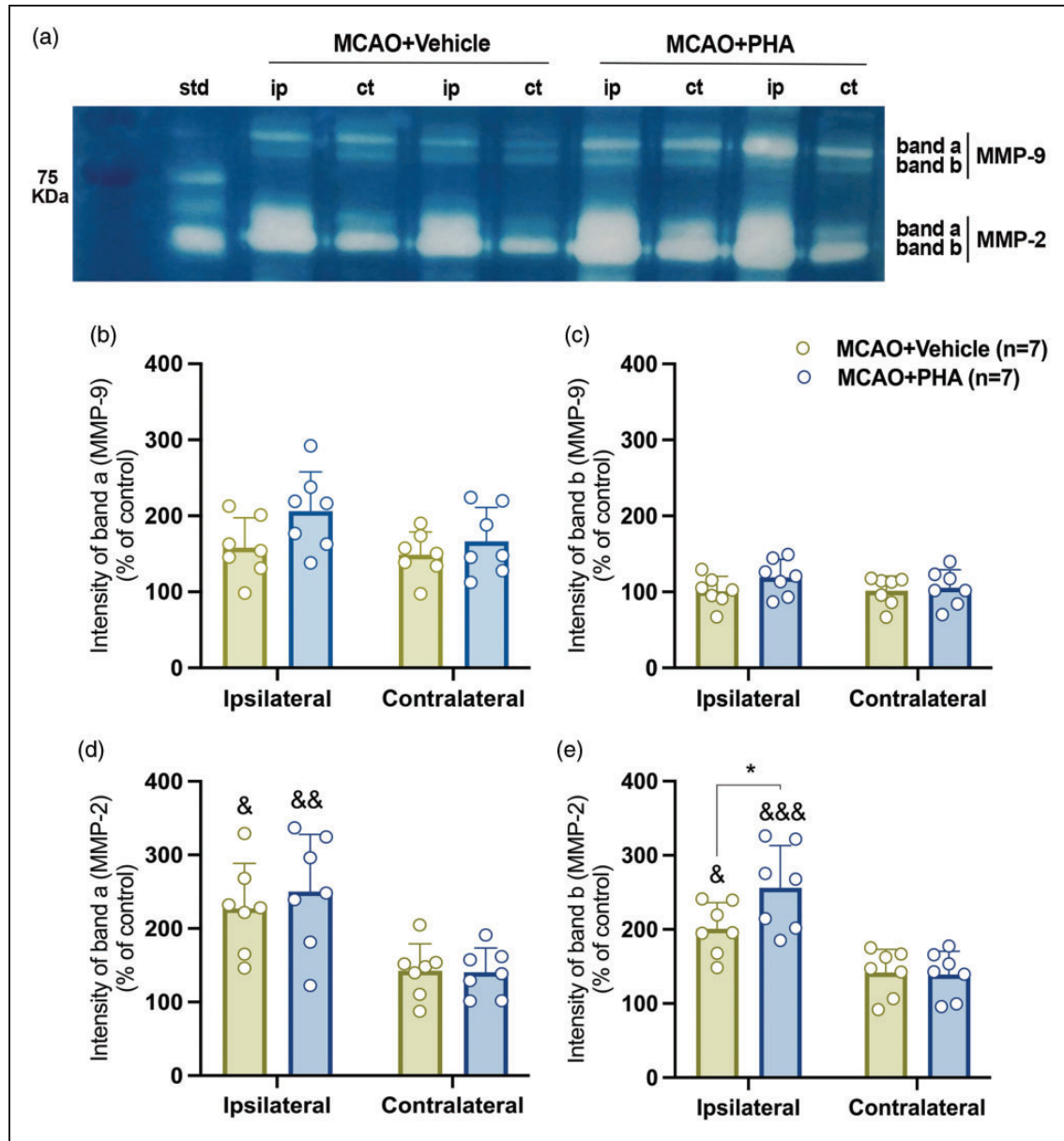
Figure 5. Gelatine zymography of MMP-2/-9 at day 7 after MCAO in vehicle and PHA-treated rats. Activity of a (proenzyme) and b (active form) bands of gelatinases MMP-9/-2 in zymogram shown as white bands in the ipsilateral and contralateral hemispheres after ischemia (a). Intensity of bands a (b, d) and bands b (c, e) of MMP-2/-9 were quantified in both ipsilateral and contralateral hemispheres after MCAO. *$p < 0.05$ compared with vehicle; $^{\&}p < 0.05$, $^{\&\&}p < 0.01$, $^{\&\&\&}p < 0.001$ compared with contralateral. Values are presented as scatter dot blot (mean $\pm$ SD).

Discussion

Although neuroprotective stroke therapies have shown to be useful in preclinical cerebral ischemia, few of them have been successfully applied in clinical practice.[18] Hence, the development of novel imaging strategies based on targeting immune biomarkers with therapeutic and prognostic value is paramount in the treatment of stroke. Because of this, we have used advanced MRI and PET techniques to evaluate the

therapeutic properties of $\alpha 7$ nAChRs on brain damage outcome, neuroinflammatory reaction, protease activation and blood vascular integrity during acute and subacute preclinical ischemic stroke.

Therapeutic effect of $\alpha 7$ nAChRs activation following cerebral ischemia

A previous study from our group evaluated the therapeutic properties of the daily treatment with the
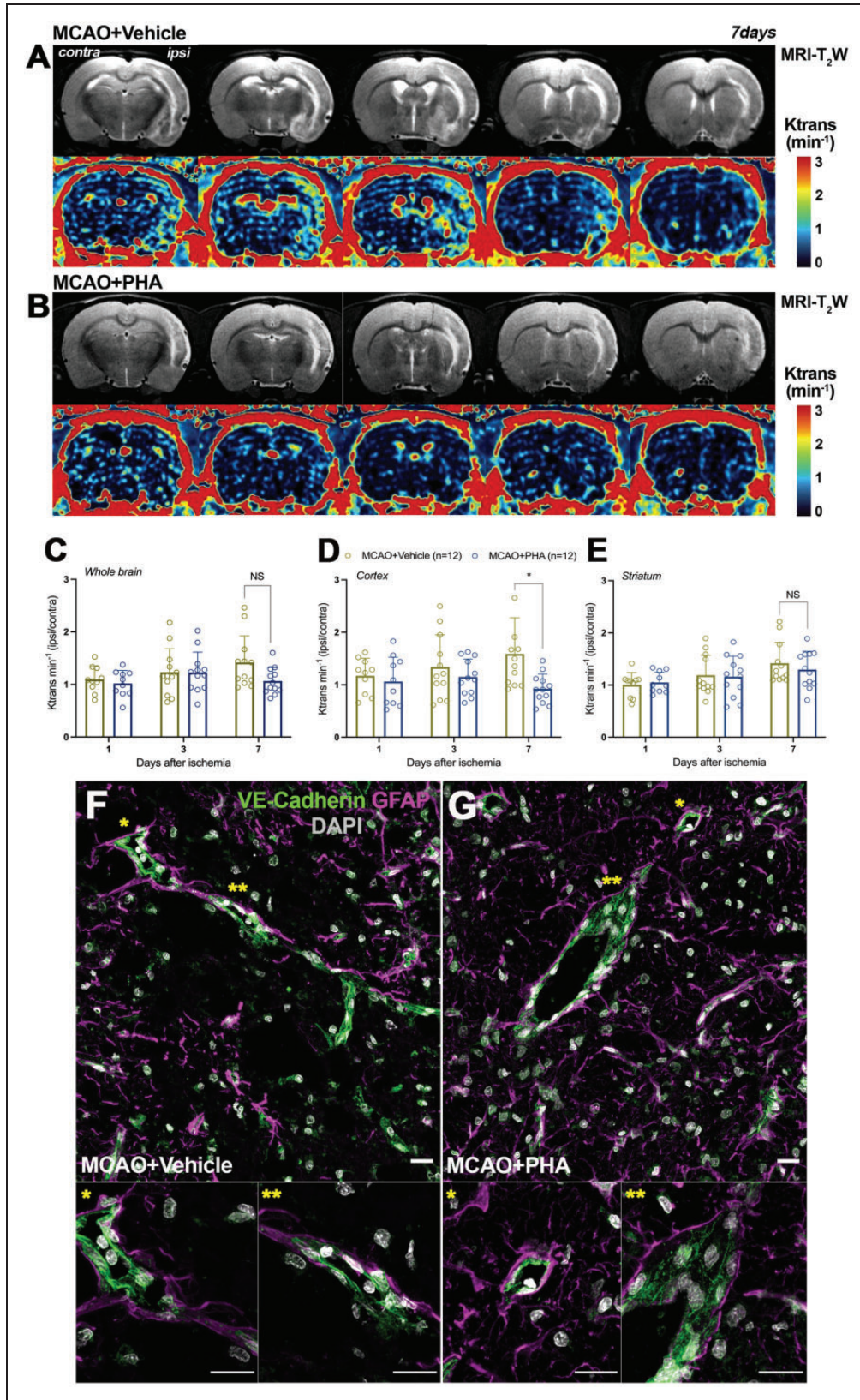
Figure 6. MRI-T_2W and DCE-MRI images at day 7 after MCAO in vehicle and PHA-treated rats. MRI axial images show the ischemic lesion and blood brain barrier disruption (BBBd) (Ktrans) at the level of the lesion (a, b). Ktrans was quantified at days 1, 3 and 7 after ischemia in the whole brain (c) cortex (d) and striatum (e). Immunofluorescent merged images of VE-Cadherin (green), GFAP (pink) and DAPI (white) in the ischemic cerebral cortex at day 7 after vehicle (f) and PHA-treated ischemic rats (g). *p < 0.05 compared with vehicle. Scale bars, 20 μm. Values are presented as scatter dot blot (mean ± SD).

selective α7 nAChR agonist PHA 568487 during 6 consecutive days, starting at day 1 following MCAO. This study evaluated the neurological outcome and stroke evolution before (at day 1) and at 7 days after ischemia showing a significant neurofunctional improvement and stroke volume reduction at the end of PHA treatments.[6] In the present study, ischemic rats were treated 7 consecutive days, starting at 1 hour following MCAO to evaluate the effect of early treatment on stroke outcome at acute (day 1) and sub-acute (days 3 and 7) cerebral ischemia. Similar to late start of treatment, PHA administration during early reperfusion (1 hour) did not show a significant improvement on neurological impairment, stroke volume and midline displacement at day 1 after MCAO (Figure 1). Nevertheless, the activation of α7 nicotinic receptors rescued ischemic damage showing a neurological, brain infarction and intracranial pressure improvement during subacute ischemic stroke (3 to 7 days) in relation to vehicle-treated ischemic rats (Figure 1(b) to (f)). In fact, these findings support those described by Zou and colleagues who observed a brain oedema reduction in ischemic mice treated with PHA 568487.[8] One possible mechanism to explain the therapeutic protection of α7 nAChRs against brain ischemic damage might be the improvement of neuronal survival and inhibition of neuronal pyroptosis by increasing neuroprotective effects of endogenous choline/Ach through vagus nerve stimulation.[19,20] In agreement with these studies, we observed a significant reduction in the number of Fluoro-Jade positive neurodegenerative cells as result of pharmacological treatment with PHA at day 7 following ischemia (Figures 1(g) to (i)).

α7 nAChRs activation attenuates neuroinflammation after ischemia

The "inflammatory reflex", considered as the complex interactions between the nervous and immune system, is still a poorly understood biological process. However, it seems clear that the anti-inflammatory response followed by vagal stimulation is mediated by the activation of α7 nAChRs.[21,22] In fact, the activation of cholinergic anti-inflammatory pathway using α7 nAChR ligands has shown potential as a strategy to control the peripheral inflammatory response in stroke patients.[5,23] Recently, Gaidhani and colleagues have observed that the effect of α7nAChRs on neuroinflammatory reaction is driven by the expression increase of these receptors in the brain and not peripherally through the spleen.[24] Hence, overexpression of these receptors in microglia and infiltrated macrophages at the region of the infarction from days 3 to 7 after MCAO might be the responsible for the

cholinergic anti-inflammatory response after ischemia.[6] Previously, the pharmacological activation of α7-nAChRs with the agonist PHA 568487 has shown a reduction in neuroinflammation following cerebral ischemia in rodents.[25,26] In our study, we explored the effect of PHA on cerebral inflammation with [^{18}F] DPA-714-PET (TSPO) and brain oedema using T_2W-MRI at days 1, 3 and 7 after MCAO (Figures 2(a) to (d)). Cerebral ischemia induced a progressive significant increase of *in vivo* neuroinflammation as observed with PET from days 1 to 7 after ischemia in the ipsilateral whole brain, cerebral cortex and striatum. Indeed, the effect of PHA showed a significant decrease of TSPO expression at day 7 in the whole ischemic hemisphere and particularly in the cerebral cortex compared to striatum (Figures 2(e), (g) and (f)). Therefore, these results suggest a differential therapeutic response between the brain regions most commonly affected by the MCAO model used in this work,[27] evidencing the significant reduction of the cortical neuroinflammatory penumbra by the activation of α7-nAChRs with PHA.[28] At day 7 after ischemia, ischemic rat brains displayed a significant decrease of CD11b positive cells expressing TSPO after treatment with PHA in both ischemic whole brain and cerebral cortex but not in striatum (Figure 3), confirming the results obtained with [^{18}F]DPA-714 PET and the role of α7 nAChRs on microglia/macrophages activation and other infiltrated leukocytes after cerebral ischemia in rats.

Treatment with PHA modulates MMP activation and restores BBBd after MCAO

Following cerebral ischemia, activated microglia and infiltrated leucocytes express a large amount of different matrix metalloproteinases including gelatinase-type MMP-2/-9 which are well characterized as key factors involved in brain ischemic damage.[29,30] MMPs are an extended family of zinc-dependent endopeptidases that require cleavage for enzymatic activation and play a crucial role in the degradation of the neurovascular matrix integrity contributing to the infarct extent and BBBd.[31–33] Additionally, MMPs have been closely related to some pathological features of secondary ischemic damage such as haemorrhagic transformation, brain inflammation and oedema formation.[34] *In vivo* imaging approaches evaluating the temporal and spatial dynamics of MMPs following experimental stroke have been possible due to the development of an [^{18}F]-labelled derivative of the MMP inhibitor CGS 27023 A ([^{18}F]BR-351) for PET imaging.[11,35] In our study, we observed maximum [^{18}F]BR-351 uptake levels in the infarcted striatum at 1 day after cerebral ischemia followed by a progressive significant decline

during sub-acute ischemia (days 3 and 7) (Figure 4). Nevertheless, our results stand in contrast with those observed by Zinnhardt and colleagues that showed *in vivo* MMP activation during the first 24/48 hours followed by non-significant increased values at day 7 after ischemia.[11] In fact, these discrepancies could be due to the use of different rodent species (rat vs. mouse) as well as different MCA occlusion times (75 min vs. 30 min), among others. Besides, we used this PET tracer to evaluate the effect of PHA 568487 on MMP activation after ischemia. Our results showed a significant increase of MMP activation in cerebral cortex at days 3 and 7 after MCAO as response to the treatment that was not observed in striatum (Figures 4(f) and (g)). Hence, the increase of [^{18}F]BR-351 uptake in the cerebral cortex might be in agreement with the decrease of the inflammatory reaction in this brain region after ischemia suggesting the protective role of cortical MMP activation on brain inflammation (Figures 3 and 4). Supporting these findings, gel zymography showed significant increase of both bands a (proenzyme) and b (active form) of MMP-2, but not MMP-9, in the ischemic lesion in comparison to contralateral hemisphere (Figure 5). Likewise, the treatment with PHA increased the intensity of the MMP-2 active form in relation to control rats at day 7 after experimental stroke (Figure 5(e)) supporting the increase of PET-[^{18}F]BR-351 signal after MCAO. In fact, [^{18}F]BR-351 binds to activated forms of MMP-2 ($IC_{50} = 4$ nmol/L), -8 (2 nmol/L), -9 (50 nmol/L), and -13 (11 nmol/L) and since MMP-8 and -13 have been also detected in experimental models of brain ischemia,[35–37] [^{18}F]BR-351 signal observed in this study cannot be attributed to the MMP-2 activation alone. In particular, MMP-2 and -13 have been related to neuroprotection and better stroke outcome,[32,38] and might be involved in the beneficial role of α7-nAChRs after ischemia observed in this work.

The major pathological effect of MMP activation after brain ischemia is the disruption of BBB, however a different role of both MMP-2 and -9 have been described on the biphasic opening of the BBB.[39] A reversible opening during first hours is related to MMP-2 activation followed by a more severe BBBd due to increased MMP-9 active forms which is associated with haemorrhagic transformation and vasogenic oedema.[40] In our study, we observed a progressive BBBd increase during the first week after cerebral ischemia in rats that was reverted by the daily treatment with PHA (Figure 6). This progressive increase is consistent with the increase of neuroinflammation observed by [^{18}F]DPA-714-PET during the first week after cerebral ischemia (Figure 2). Similarly, it has become more apparent that intense neuroinflammation resulting in brain injury after ischemic stroke is associated with BBB breakdown, neuronal injury, and worse neurological outcomes.[41,42] Finally, the activation of α7-nAChRs showed protection on blood brain vessel integrity and significantly reduced BBBd in the cerebral ischemic cortex at day 7 after ischemia (Figure 6(d)). Thus, these findings suggest for the first time the protective role of MMP-2 activation in the restoration of BBBd after cerebral ischemia through α7-nAChRs modulation.

Summary and conclusions

In summary, multimodal imaging studies were carried out to decipher the therapeutic role of α7-nAChRs activation after experimental stroke in rats. The daily treatment with PHA showed beneficial effects on volume of infarction, midline displacement, neurodegeneration and neurological outcome during the subacute preclinical ischemic stroke. In addition, α7-nAChRs activation reduced neuroinflammatory reaction in the cerebral cortex at day 7 after ischemia together with an increase of MMP-2 activation and the protection of the BBB and blood brain vessel integrity. Altogether, our results provide promising evidence on the therapeutic potential of α7-nAChRs activation for ischemic stroke.

Declaration of conflicting interests

The author(s) declared no potential conflicts of interest with respect to the research, authorship, and/or publication of this article.

Authors' contributions

LA, AJ, MG, SPG, LI, MIH, MA, NM, VGV, UC performed experiments and acquired data; MH, MMF, MD,

PRC, JLl, AM designed experiments; ARA, CM, PRC, JLl, AM, analysed data, prepared the manuscript and approved the final version of the manuscript.

ORCID iDs

María Ardaya https://orcid.org/0000-0002-0103-5649
Carlos Matute https://orcid.org/0000-0001-8672-711X

Supplemental material

Supplemental material for this article is available online.

References

1. Gauberti M, Martinez de Lizarrondo S and Vivien D. Thrombolytic strategies for ischemic stroke in the thrombectomy era. *J Thromb Haemost* 2021; 19: 1618–1628.

2. Chamorro Á, Dirnagl U, Urra X, et al. Neuroprotection in acute stroke: targeting excitotoxicity, oxidative and nitrosative stress, and inflammation. *Lancet Neurol* 2016; 15: 869–881.

3. Dagonnier M, Donnan GA, Davis SM, et al. Acute stroke biomarkers: are we there yet? *Front Neurol* 2021; 12: 619721.

4. Martín A, Domercq M and Matute C. Inflammation in stroke: the role of cholinergic, purinergic and glutamatergic signaling. *Ther Adv Neurol Disord* 2018; 11: 1756286418774267–.

5. Neumann S, Shields NJ, Balle T, et al. Innate immunity and inflammation post-stroke: an α7-nicotinic agonist perspective. *Int J Mol Sci* 2015; 16: 29029–29046.

6. Colás L, Domercq M, Ramos-Cabrer P, et al. In vivo imaging of A7 nicotinic receptors as a novel method to monitor neuroinflammation after cerebral ischemia. *Glia* 2018; 66: 1611–1624.

7. Kimura I, Dohgu S, Takata F, et al. Activation of the α7 nicotinic acetylcholine receptor upregulates blood-brain barrier function through increased claudin-5 and occludin expression in rat brain endothelial cells. *Neurosci Lett* 2019; 694: 9–13.

8. Zou D, Luo M, Han Z, et al. Activation of alpha-7 nicotinic acetylcholine receptor reduces brain edema in mice with ischemic stroke and bone fracture. *Mol Neurobiol* 2017; 54: 8278–8286.

9. de Jonge WJ and Ulloa L. The alpha7 nicotinic acetylcholine receptor as a pharmacological target for inflammation. *Br J Pharmacol* 2007; 151: 915–929.

10. Martín A, Boisgard R, Thézé B, et al. Evaluation of the PBR/TSPO radioligand [(18)F]DPA-714 in a rat model of focal cerebral ischemia. *J Cereb Blood Flow Metab* 2010; 30: 230–241.

11. Zinnhardt B, Viel T, Wachsmuth L, et al. Multimodal imaging reveals temporal and spatial microglia and matrix metalloproteinase activity after experimental stroke. *J Cereb Blood Flow Metab* 2015; 35: 1711–1721.

12. Joya A, Ardaya M, Montilla A, et al. In vivo multimodal imaging of adenosine A(1) receptors in neuroinflammation after experimental stroke. *Theranostics* 2021; 11: 410–425.

13. Ortuño JE, Ledesma-Carbayo MJ, Simões RV, et al. DCE@urLAB: a dynamic contrast-enhanced MRI pharmacokinetic analysis tool for preclinical data. *BMC Bioinformatics* 2013; 14: 316.

14. Dobre MC, Uğurbil K and Marjanska M. Determination of blood longitudinal relaxation time (T1) at high magnetic field strengths. *Magn Reson Imaging* 2007; 25: 733–735.

15. Pulagam KR, Colás L, Padro D, et al. Evaluation of the novel TSPO radiotracer [(18)F] VUIIS1008 in a preclinical model of cerebral ischemia in rats. *EJNMMI Res* 2017; 7: 93.

16. Vazquez N, Missault S, Vangestel C, et al. Evaluation of [(18) F]BR420 and [(18) F]BR351 as radiotracers for MMP-9 imaging in colorectal cancer. *J Labelled Comp Radiopharm* 2017; 60: 69–79.

17. Pérez-Asensio FJ, Hurtado O, Burguete MC, et al. Inhibition of iNOS activity by 1400W decreases glutamate release and ameliorates stroke outcome after experimental ischemia. *Neurobiol Dis* 2005; 18: 375–384.

18. Kim JH, Kim SY, Kim B, et al. Prospects of therapeutic target and directions for ischemic stroke. *Pharmaceuticals (Basel)* 2021; 14 : 20210401.

19. Kalappa BI, Sun F, Johnson SR, et al. A positive allosteric modulator of α7 nAChRs augments neuroprotective effects of endogenous nicotinic agonists in cerebral ischaemia. *Br J Pharmacol* 2013; 169: 1862–1878.

20. Tang H, Li J, Zhou Q, et al. Vagus nerve stimulation alleviated cerebral ischemia and reperfusion injury in rats by inhibiting pyroptosis via α7 nicotinic acetylcholine receptor. *Cell Death Discov* 2022; 8: 54.

21. Martelli D, McKinley MJ and McAllen RM. The cholinergic anti-inflammatory pathway: a critical review. *Auton Neurosci* 2014; 182: 65–69.

22. Wang H, Yu M, Ochani M, et al. Nicotinic acetylcholine receptor alpha7 subunit is an essential regulator of inflammation. *Nature* 2003; 421: 384–388.

23. Cai PY, Bodhit A, Derequito R, et al. Vagus nerve stimulation in ischemic stroke: old wine in a new bottle. *Front Neurol* 2014; 5: 107.

24. Gaidhani N, Kem WR and Uteshev VV. Spleen is not required for therapeutic effects of 4OH-GTS-21, a selective α7 nAChR agonist, in the sub-acute phase of ischemic stroke in rats. *Brain Res* 2021; 1751: 147196.

25. Han Z, Li L, Wang L, et al. Alpha-7 nicotinic acetylcholine receptor agonist treatment reduces neuroinflammation, oxidative stress, and brain injury in mice with ischemic stroke and bone fracture. *J Neurochem* 2014; 131: 498–508.

26. Han Z, Shen F, He Y, et al. Activation of α-7 nicotinic acetylcholine receptor reduces ischemic stroke injury through reduction of pro-inflammatory macrophages and oxidative stress. *PLoS One* 2014; 9: e1057112 0140826.

27. Buscemi L, Price M, Bezzi P, et al. Spatio-temporal overview of neuroinflammation in an experimental mouse stroke model. *Sci Rep* 2019; 9: 507.

28. Gauberti M, De Lizarrondo SM and Vivien D. The "inflammatory penumbra" in ischemic stroke: from

clinical data to experimental evidence. *Eur Stroke J* 2016; 1: 20–27.

29. del Zoppo GJ, Milner R, Mabuchi T, et al. Microglial activation and matrix protease generation during focal cerebral ischemia. *Stroke* 2007; 38: 646–651.

30. Justicia C, Panés J, Solé S, et al. Neutrophil infiltration increases matrix metalloproteinase-9 in the ischemic brain after occlusion/reperfusion of the middle cerebral artery in rats. *J Cereb Blood Flow Metab* 2003; 23: 1430–1440.

31. Heo JH, Lucero J, Abumiya T, et al. Matrix metalloproteinases increase very early during experimental focal cerebral ischemia. *J Cereb Blood Flow Metab* 1999; 19: 624–633.

32. Rosell A, Ortega-Aznar A, Alvarez-Sabín J, et al. Increased brain expression of matrix metalloproteinase-9 after ischemic and hemorrhagic human stroke. *Stroke* 2006; 37: 1399–1406.

33. Wang X, Lee SR, Arai K, et al. Lipoprotein receptor-mediated induction of matrix metalloproteinase by tissue plasminogen activator. *Nat Med* 2003; 9: 1313–1317.

34. Fujimoto M, Takagi Y, Aoki T, et al. Tissue inhibitor of metalloproteinases protect blood-brain barrier disruption in focal cerebral ischemia. *J Cereb Blood Flow Metab* 2008; 28: 1674–1685.

35. Wagner S, Breyholz HJ, Höltke C, et al. A new 18F-labelled derivative of the MMP inhibitor CGS 27023A for PET: radiosynthesis and initial small-animal PET studies. *Appl Radiat Isot* 2009; 67: 606–610.

36. Han JE, Lee EJ, Moon E, et al. Matrix metalloproteinase-8 is a novel pathogenetic factor in focal cerebral ischemia. *Mol Neurobiol* 2016; 53: 231–239.

37. Ma F, Martínez-San Segundo P, Barceló V, et al. Matrix metalloproteinase-13 participates in neuroprotection and neurorepair after cerebral ischemia in mice. *Neurobiol Dis* 2016; 91: 236–246.

38. Lucivero V, Prontera M, Mezzapesa DM, et al. Different roles of matrix metalloproteinases-2 and -9 after human ischaemic stroke. *Neurol Sci* 2007; 28: 165–170.

39. Rosenberg GA. Matrix metalloproteinases in neuroinflammation. *Glia* 2002; 39: 279–291.

40. Rosenberg GA, Estrada EY and Dencoff JE. Matrix metalloproteinases and TIMPs are associated with blood-brain barrier opening after reperfusion in rat brain. *Stroke* 1998; 29: 2189–2195.

41. Candelario-Jalil E, Dijkhuizen RM and Magnus T. Neuroinflammation, stroke, blood-brain barrier dysfunction, and imaging modalities. *Stroke* 2022; 53: 1473–1486.

42. Yang C, Hawkins KE, Doré S, et al. Neuroinflammatory mechanisms of blood-brain barrier damage in ischemic stroke. *Am J Physiol Cell Physiol* 2019; 316: C135–C153.